Iterative Blind Deconvolution of Extended Objects

David S. C. Biggs and Mark Andrews
Department of Electrical and Electronic Engineering
The University of Auckland, Auckland, New Zealand
Email: {dsc.biggs, m.andrews}@auckland.ac.nz

Abstract

This paper describes a technique for the blind deconvolution of extended objects such as Hubble Space Telescope (HST), scanning electron and 3D fluorescence microscope images. The blind deconvolution mechanism is based on the Richardson–Lucy algorithm and alternates between deconvolution of the image and point spread function (PSF). This form of iterative blind deconvolution differs from that typically employed in that multiple PSF iterations are performed after each image iteration. The initial estimate for the PSF is the autocorrelation of the blurred image and the edges of the image are windowed to minimise wrap around artifacts. Acceleration techniques are employed to speed restoration and results from real HST, electron microscope and 3D fluorescence images are presented.

1 Introduction

The desire to remove distortion introduced by a spatially invariant point spread function (PSF) is a challenge faced in many imaging applications. The observed image, $g(x,y)$, results from the convolution ($\otimes$) of the true image, $f(x,y)$, with the distorting PSF, $h(x,y)$, plus contamination, $c(x,y)$, from any number of sources:

$$g(x,y) = f(x,y) \otimes h(x,y) + c(x,y) \qquad (1)$$

Blind deconvolution (BD) algorithms are predominately iterative and attempt to recover both the image and PSF from a blurred observation using a variety of constraints such as non–negativity and object support.

One family of algorithms use standard deconvolution methods to alternate between restoration of the image and PSF. This form of *grouped coordinate descent* [1] is typically referred to as iterative blind deconvolution (IBD) and has been popularised by Ayers and Dainty [2] and extended using a Weiner filter by Davey et. al [3]. The images in the literature typically restored using these techniques are binary test images, blurry stars and speckle imagery [4]. This paper proposes an algorithm for the restoration of real world extended grayscale objects such as planetary and microscopy images.

2 Blind Deconvolution Method

A generic IBD method is shown in Figure 1. One variable is fixed while the other is updated and, as in [5] and [6], an RL iteration is employed to achieve this. However the major difference introduced in this paper is that multiple PSF iterations are applied after each image iteration. This is necessary because the image estimate converges faster than the PSF due to differences in their extent. The RL algorithm [7, 8] for updating $f_k(x,y)$ can be written as:

$$f_{k+1}(x,y) = f_k(x,y) \cdot \left(h_k(x,y) \star \frac{g(x,y)}{r_k(x,y)} \right) \qquad (2)$$

$$r_k(x,y) = f_k(x,y) \otimes h_k(x,y) \qquad (3)$$

where $r_k(x,y)$ is termed the reblurred image and $\star$ is the correlation operator.

The initial PSF estimate is based upon the autocorrelation of the blurred data — the result of applying

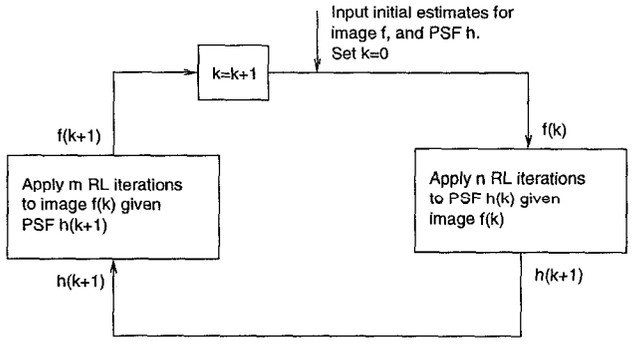

Figure 1: Blind deconvolution by iterating between image and PSF estimates.

0-8186-8183-7/97 $10.00 © 1997 IEEE

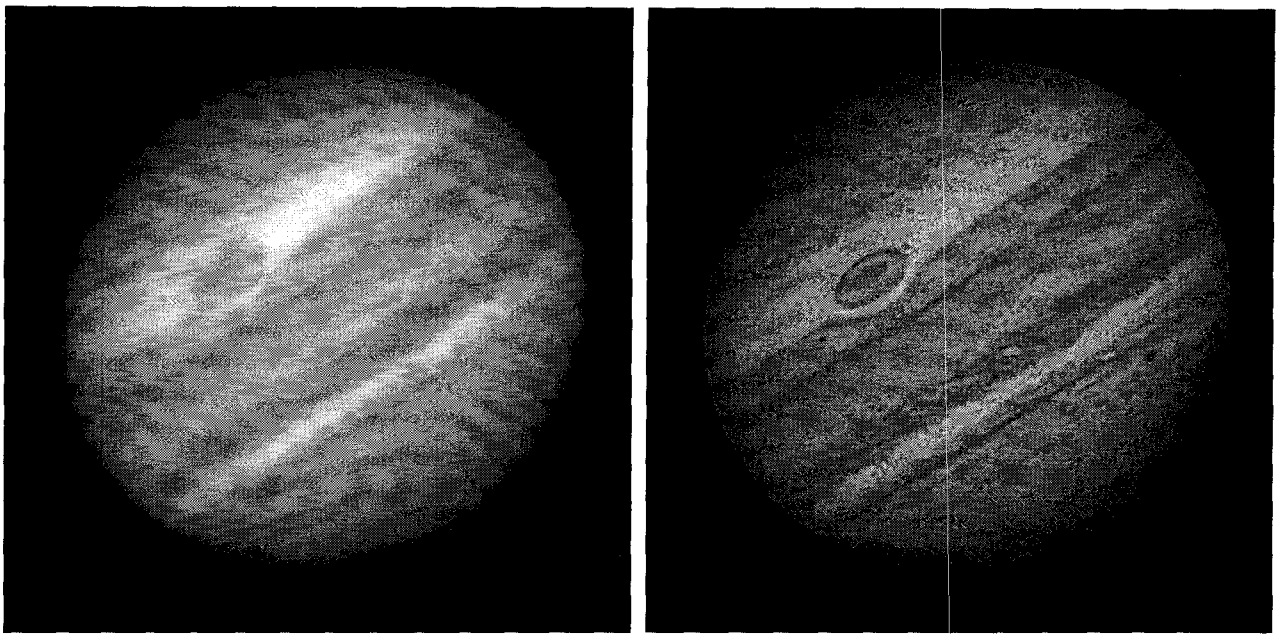

(a) (b)

Figure 2: (a) Blurred Hubble image of Jupiter, (b) blind deconvolution after 60 accelerated cycles.

one RL iteration to a constant valued PSF estimate with the blurred data as the image estimate. The autocorrelation is adjusted to minimise the DC offset while maintaining non–negativity and normalised to unit volume. Choosing the number of PSF iterations to apply after each iteration iteration is currently experimental though methods to automate this are being actively researched.

The RL algorithm is a maximum likelihood approach employed when the contaminating noise has Poisson statistics. If the noise has Gaussian statistics then a least squares method can be employed:

$$f_{k+1}(x,y) = f_k(x,y) + h_k(x,y) \star (g(x,y) - r_k(x,y)) \quad (4)$$

however non–negativity is not guaranteed [9].

To speed restoration an acceleration technique is applied to the image and PSF estimates after each iteration [10, 11]. The algorithm from [11] is employed and produces a significant speedup without requiring an additional optimisation step.

2.1 Dealing with Boundaries

In applications such as scanning electron microscopy (SEM) the object often extends beyond the observed image boundaries. When using the FFT the edges must be considered to prevent wrap around discontinuities. The proposed solution is, after each iteration, to window the reblurred image, $r_k(x,y)$, and compensate with the known blurred data, thus reducing the edge effects:

$$\hat{r}_k(x,y) = r_k(x,y) \cdot w(x,y) + (1 - w(x,y)) \cdot g(x,y) \quad (5)$$

where $w(x,y)$ is the windowing function, the type and size of the which depends upon the image and PSF. A general purpose method is to use a Hanning function, though more advanced techniques can dynamically adjust the window based upon the current PSF estimate. It should be noted that data within the windowed region is not fully deconvolved.

3 Results

3.1 Hubble Space Telescope

A blurred Hubble Space Telescope (HST) image of Jupiter (dataset W0VI0207T) is shown in Figure 2a. The restoration, after 60 cycles with 10 PSF iterations for each image iteration, is shown in Figure 2b. The only constraint on the solution is non–negativity which the RL algorithm automatically preserves. The edge effects are ignored as the object does not extend beyond the borders of the image.

The restored image shows significantly more detail than the blurred image with no visible artifacts and compares favourably with the results given in [12].

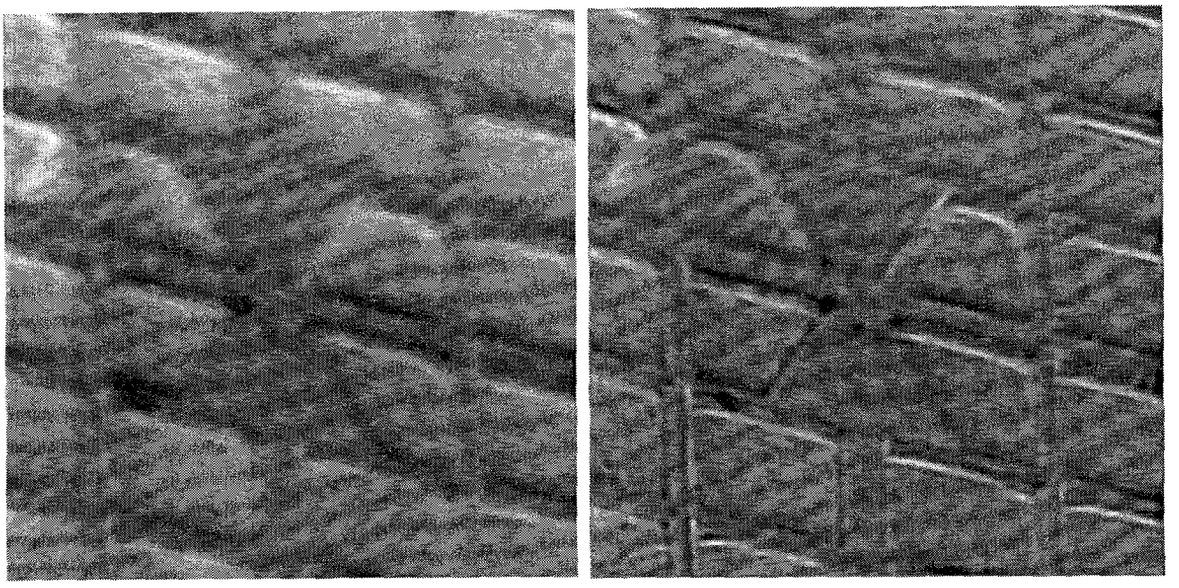

(a) (b)

Figure 3: (a) Out of focus SEM image, (b) result after 50 accelerated IBD cycles with symmetry constraint on PSF.

3.2 Scanning Electron Microscopy

In SEM, blurring can occur due to the non–ideal profile of the electron beam. Distortion can be caused by spherical or chromatic aberration, astigmatism and defocus [13], and the difficulty in estimating these effects limits accurate modelling of the PSF.

Figure 3a shows an out-of-focus SEM image of a copper grid pressed into indium that extends beyond the edges. Figure 3b is the result of 50 cycles of the IBD algorithm with edge windowing employed. A Hanning window is used within 16 pixels of the edge, otherwise $w(x, y)$ is unity.

A further modification during this restoration is that the number of PSF iterations reduces linearly from initially 10 to 1 after 50 cycles, a total of 325 RL iterations. This is possible because as the PSF converges to its final form fewer modifications are required relative to updating the image. The beam profile was also assumed to have quadrantal symmetry, which was a constraint imposed by ensuring the Fourier transform of the PSF had zero phase. The restored image has sharper edges and reveals finer detail.

3.3 3D Fluorescence Microscopy

In fluorescence microscopy light is focused on a particular plane in a 3D specimen labelled with a fluorescent marker. However out of focus light passing through planes above and below results in a conic shaped PSF which causes blurring. The PSF can be estimated by imaging a fluorescent bead under the same conditions or by using a theoretical model — however they rarely match experimental practicalities. To achieve blind deconvolution, many algorithms require information about the experimental setup to place constraints on the spatial and spectral extent of the PSF [14]. In this paper no such information is required to achieve a restoration though it can be incorporated to improve the result.

The following example is a fluorescence dataset of a nerve axon, composed of 24 serial sections each 256 by 256 pixels (original data courtesy of Vaytek, Inc). A 3D FFT was used to calculate the convolutions and a total of 130 RL iterations were performed after 30 cycles. The original and restored images shown in Figure 4a and 4b respectively are maximum intensity projections in the xy, xz and yz planes. The algorithm has successfully extracted the central core of the PSF, however some of the conic features remain. An improved result is only possible with more *a priori* information about the imaging conditions, which was unavailable in this case.

The same procedure can been used to successfully deconvolve noisy confocal microscope datasets. A confocal microscope is able to reject most out-of-focus light reducing the conic features in the PSF, but some enhancement is still possible. Confocal images are often noisy because rejecting significant unfocused light reduces the number of photons detected. Longer integra-

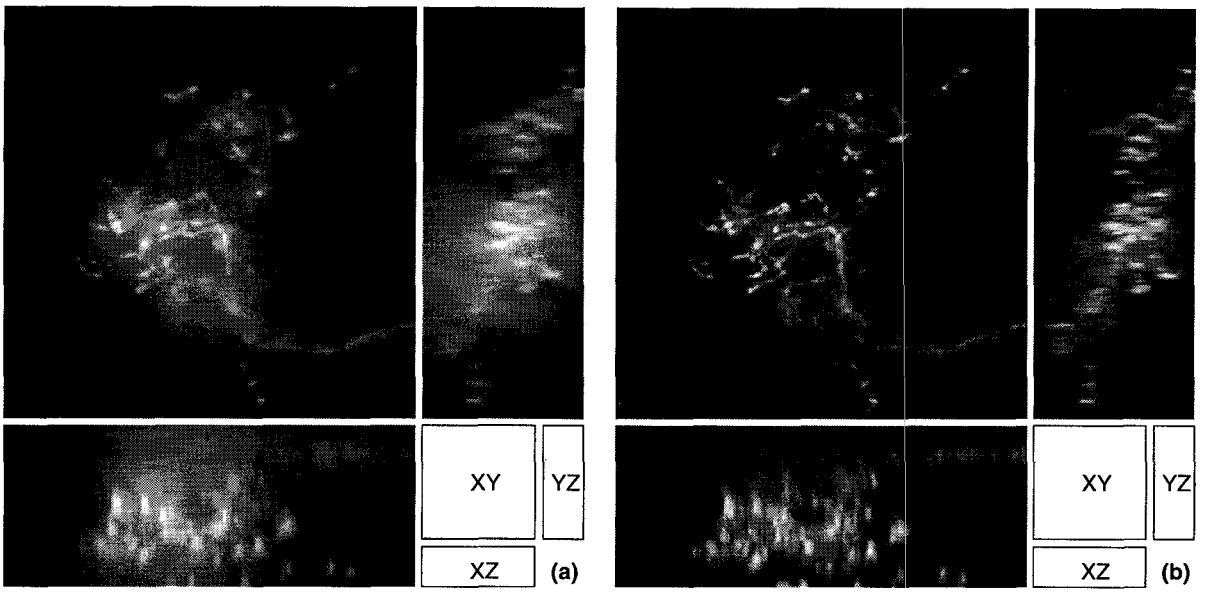

Figure 4: Maximum intensity projection of 3D fluorescence datasets, (a) original, (b) 30 accelerated IBD cycles.

tion times are thus required to improve the signal–to–noise ratio, but this may be limited by photo bleaching in the sample [15].

4 Conclusion

A modification to the IBD technique has been introduced where multiple PSF iterations are performed after each image iteration. This has been shown to successfully restore extended objects without additional spatial or spectral constraints. Edge discontinuities are minimised by windowing the boundaries. Deconvolved images from the HST and scanning electron and fluorescence microscopes have been presented.

References

[1] J. C. Bezdek, R. J. Hathaway, and R. E. Howard. Local Convergence Analysis of a Grouped Variable Version of Coordinate Descent. *J. of Optimization Theory and Applications*, 54(3):471–477, September 1987.

[2] G. R. Ayers and J. C. Dainty. Iterative Blind Deconvolution Method and its Applications. *Optics Letters*, Vol. 13(No. 7):547–549, July 1988.

[3] B. L. A. Davey, R. G. Lane, and R. H. T. Bates. Blind Deconvolution of Noisy Complex–Valued Image. *Optics Comms*, Vol. 69(No. 5,6):353–356, January 1989.

[4] R. G. Lane. Blind deconvolution of speckle images. *J. Opt. Soc. Am. A*, 9(9):1508–1514, September 1992.

[5] D.A. Fish, A. M. Brinicombe, E. R. Pike, and J. G. Walker. Blind deconvolution by means of the Richardson-Lucy algorithm. *J. Opt. Soc. Am. A*, Vol. 12(No. 1):58–65, January 1995.

[6] F. Tsumuraya, N. Miura, and N. Baba. Iterative blind deconvolution method using Lucy's algorithm. *Astronomy and Astrophysics*, 282:699–708, 1994.

[7] William H. Richardson. Bayesian-based iterative method of image restoration. *J. Opt. Soc. Am.* , Vol. 62(No. 1):55–59, January 1972.

[8] L. B. Lucy. An iterative technique for the rectification of observed images. *The Astronomical J.* , Vol. 79(No. 6):745–754, June 1974.

[9] M. Bertero, F. Maggio, E.R. Pike, and D. Fish. Assessment of Methods Used for HST Image Reconstruction. In R. J. Hanisch and R. L. White, editors, *The Restoration of HST Images and Spectra II.* Space Telescope Science Institute, 1994.

[10] D. S. C. Biggs and M. Andrews. Conjugate gradient acceleration of maximum-likelihood image restoration. *Electronics Letters*, Vol. 31(No. 23):1985–1986, 9th November 1995.

[11] D. S. C. Biggs and M. Andrews. Acceleration of Iterative Image Restoration Algorithms. *Applied Optics*, Vol. 36(No. 5):1766–1775, March 1997.

[12] Deepa Kundur and Dimitrios Hatzinakos. Blind Image Deconvolution. *IEEE Signal Processing Magazine*, Vol. 13(No. 3):43–64, May 1996.

[13] John C. H. Spence. *Experimental high-resolution electron microscopy.* Oxford University Press, New York, 2nd edition, 1988.

[14] T. J. Holmes et. al. *Handbook of Biological Confocal Microscopy*, Light Microscopic Images Reconstructed by Maximum Likelihood Deconvolution, pages 389–402. Plenum Press, New York, 1995.

[15] Peter J. Shaw. *Handbook of Biological Confocal Microscopy*, Comparison of Wide–Field/Deconolution and Confocal Microscopy for 3D Imaging, pages 373–387. Plenum Press, New York, 1995.